Supporting Information

Plasmonic Color Palettes for Photorealistic Printing with Aluminum Nanostructures

Shawn J. Tan[1], *Lei Zhang*[2], *Di Zhu*[1], *Xiao Ming Goh*[1], *Ying Min Wang*[1], *Karthik Kumar*[1,†], *Cheng-Wei Qiu*[2], *Joel K.W. Yang*[1,3,*]

[1] Institute of Materials Research and Engineering, A*STAR, 3 Research Link, Singapore 117602, Singapore

[2] Department of Electrical and Computer Engineering, National University of Singapore, 4 Engineering Drive 3, Singapore 117583, Singapore

[3] Singapore University of Technology and Design, Singapore 138682, Singapore

[†] Current Address: Biomedical Research Council, A*STAR, Singapore

[*] Corresponding Email: joel_yang@sutd.edu.sg

KEYWORDS: Nanoplasmonics, Aluminum plasmonics, Color printing, Structural color, Electron-beam lithography

Materials and Methods

Electron-beam lithography (EBL). Negative-tone electron-beam resist HSQ (Product number: XR-1541-006, Dow Corning, Michigan, USA) was spin-coated onto silicon substrates to a thickness of 95 nm. No baking process was applied on the resist layers so as to avoid thermally-induced crosslinking of the resist, thus enabling a higher resolution of patterning to be achieved. EBL was performed using an Elionix ELS-7000 EBL system (Elionix Inc., Tokyo, Japan) with an accelerating voltage of 100 kV and a beam current of 500 pA. The write field was set to 150 μm × 150 μm with and exposure step size of 2.5 nm. The dose used for patterning the nanodisk structures was 12 mC cm^{-2}. No proximity-effect correction was performed for the exposure. Instead, to achieve well-defined nanodisk structures with steep sidewalls, a high-contrast development process – samples were developed in a formulation of aqueous 1% NaOH, 4% NaCl in deionized (DI) water at 24^{o}C for 1 min, followed by rinsing under running DI water for 2 min.[1] The developed samples were then blow-dried under a steady stream of N_2.

Pattern generation. MATLAB (The Mathworks Inc., Massachusetts, USA) was used to generate a layout consisting of arrays of nanostructures with a range of diameters, pitch, shape and gaps for electron-beam lithography. No software-based proximity-effect correction was performed on the layouts. For the demonstration of plasmonic color paintings, we used a digital copy of a Monet painting (*Impression, Sunrise*) that is already in the public domain and not bound by copyright laws, from Wikipaintings (URL: www.wikipaintings.org). The digital copy was input into MATLAB and the color of each pixel was matched to a corresponding pixel layout, and finally output into an overall layout for EBL.

Metal deposition. Metal deposition was performed using an electron-beam evaporator system (Explorer Coating System, Denton Vacuum Inc., New Jersey, USA). An aluminum plasmon-active layer (20 nm) was deposited onto the developed samples at a rate of 1 $Å s^{-1}$. The working pressure during evaporation was ~1×10^{-6} torr. The temperature of the sample chamber was maintained at $20^{o}C$ during the entire evaporation process, with the sample holder rotating at a rate of 50 rpm to ensure uniformity of the deposition. The fabricated structures were imaged using an Elionix ESM-9000 scanning electron microscope (Elionix Inc., Tokyo, Japan) with an accelerating voltage of 10 kV and a working distance of 5 mm.

Optical measurements. To investigate the optical properties of the fabricated structures, extinction spectra were measured in reflection mode using a QDI 2010 UV-visible-NIR range microspectrophotometer (CRAIC Technology Inc., California, USA). Both incident and collected light were at normal incidence to the substrate, with the electric field of the linearly polarized light in plane with the substrate surface. Optical micrographs were acquired using a Olympus MX61 (Olympus Inc., Tokyo, Japan) set-up with ×5 (0.15 NA), ×10 (0.3 NA), ×20 (0.45 NA), ×50 (0.8 NA) and ×150 (0.9 NA) air objectives, using a SC30 Olympus Digital Camera. ImageJ (NIH, Maryland, USA) was used to process optical images in the form of resizing and/or background normalization for the purpose of comparison.

Numerical simulations. Finite-difference time-domain (FDTD) simulations were performed using commercial software (Lumerical FDTD Solutions). Individual pixels with different disk diameters and inter-pitch distances were simulated. The single pixel, consisting of 4 disks, was surrounded by perfectly-matched layers, and illuminated with normal incident plane waves using a total field scattered field (TFSF) source . The electric field was polarized along the center-to-center axis of two adjacent nanopillars, i.e. in the x-z plane as indicated in Figure 3C and 3D.

Reflection spectra were calculated by subtracting the absorption and transmission from the total incident power. The complex refractive indices of aluminum and silicon were taken from literature[2], and the refractive index for HSQ was simulated as a constant of 1.41.

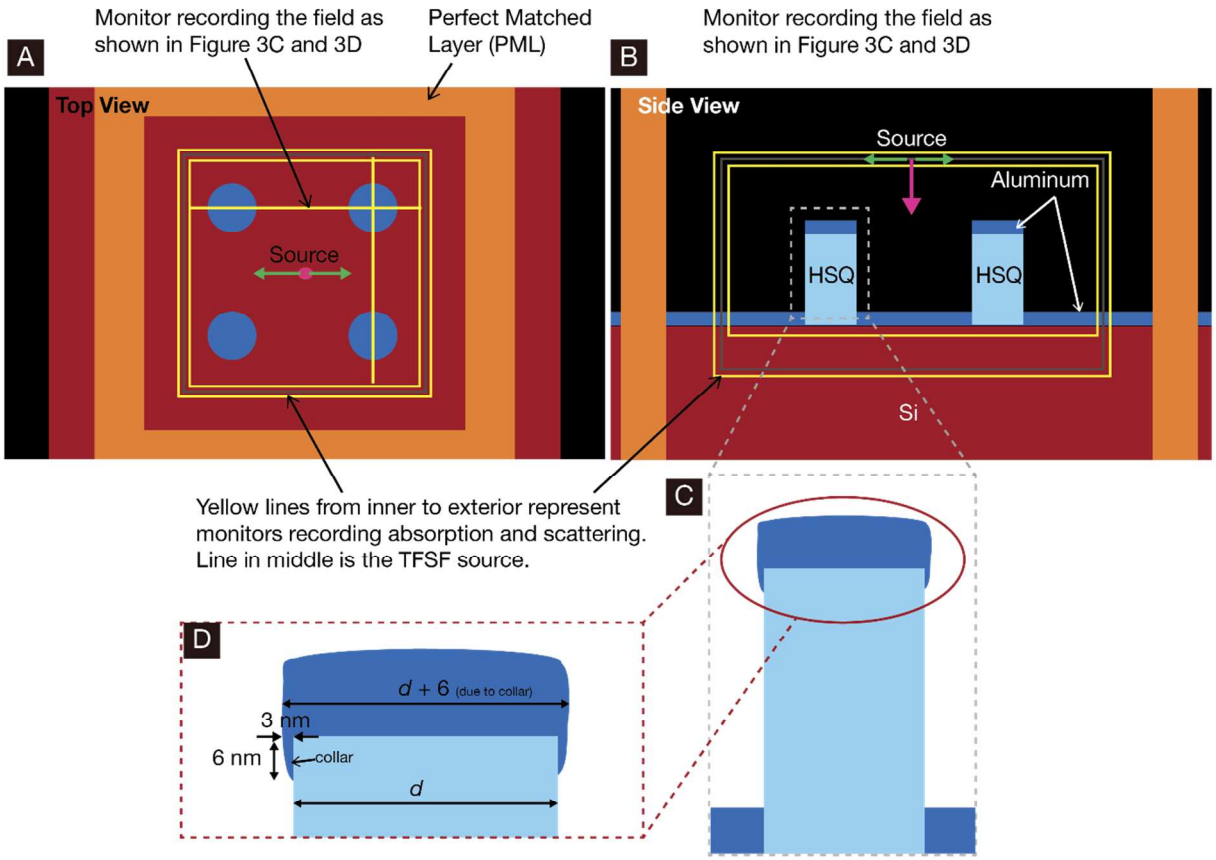

Figure S1. Simulation setup used for FDTD simulations from a (A) top view and (B) side view. Based on the SEM results shown in Fig. S3, the aluminum nanodisks were modeled with an extended collar (overcoat) of ~ 3 nm around the HSQ nanopillar as show in (C) and (D).

Durability of Aluminum Plasmonic Colors

An aluminum color palette was fabricated in the same process detailed in the manuscript and imaged under an optical microscope. The same color palette was imaged 224 days later after being left out in ambient conditions (Figure S2). There was a slight increase in minor color variations that was observable only at a high magnification of 150×. Overall, the aluminum colors remained remarkably similar 224 days later, highlighting the durability and robustness of

the aluminum plasmonic color palettes. In comparison, silver color palettes exhibited visible signs of degradation within a week due to oxidation and sulfidation of the silver metal (data not shown).

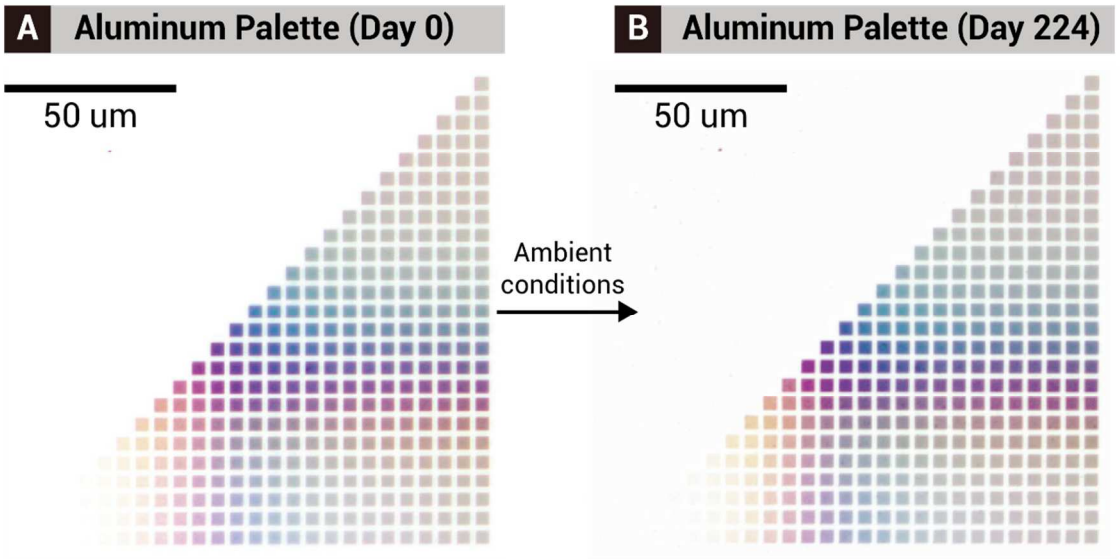

Figure S2. Optical images of the same aluminum palette upon fabrication (Day 0) and after seven months (Day 224) show a high degree of color retention, highlighting the durability and robustness of aluminum palettes. The optical images were normalized to a white background for comparison.

Height of Nanopillars

A color palette with aluminum nanodisks evaporated onto HSQ nanopillars was mechanically agitated, resulting in collapsed nanopillars. The height of these collapsed nanostructures was measured using SEM to be ~ 115 nm, which is consistent with a 20 nm layer of aluminum evaporated onto a 95 nm patterned HSQ resist layer (Figure S3). The collapsed nanopillars also revealed the formation of an aluminum collar around the top edges of the HSQ nanopillar, due to sidewall deposition during metal evaporation. This collar was measured to be ~ 3 nm thick,

extending ~ 6 nm down from the HSQ-aluminum interface. This feature was taken account in our FDTD simulations.

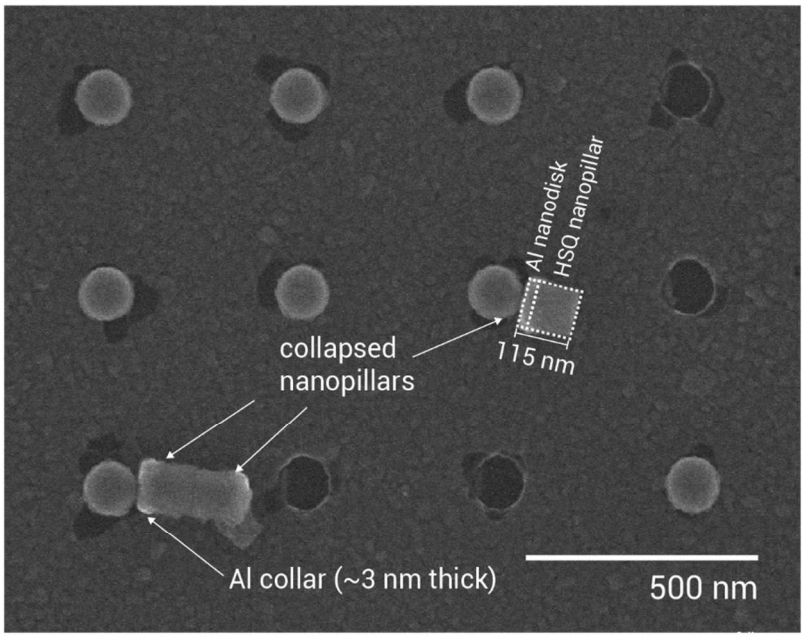

Figure S3. Collapsed nanostructures of aluminum nanodisks sitting atop HSQ nanopillars obtained by mechanical agitation revealed that the height of the nanostructures was ~ 115 nm through SEM characterization. Note that the bottom left structure shows two collapsed nanopillars that are coincidentally joint at the ends.

Resolution of a Single Pixel

A single pixel containing four aluminum nanodisks can be resolved amidst an array of pixels corresponding to a single color as shown in Figure S3. Figure S3C indicates that the colors manifested by individual aluminum nanodisks within the pixel can also be resolved under an optical microscope, at diameter steps of 20 nm. In addition, minor random variations in color were observed in the background with nanodisk diameters of 100 nm, likely arising from the fabrication process. This also highlights the sensitivity of plasmonic colors to structural parameters, which is consistent with what have been widely reported in literature.

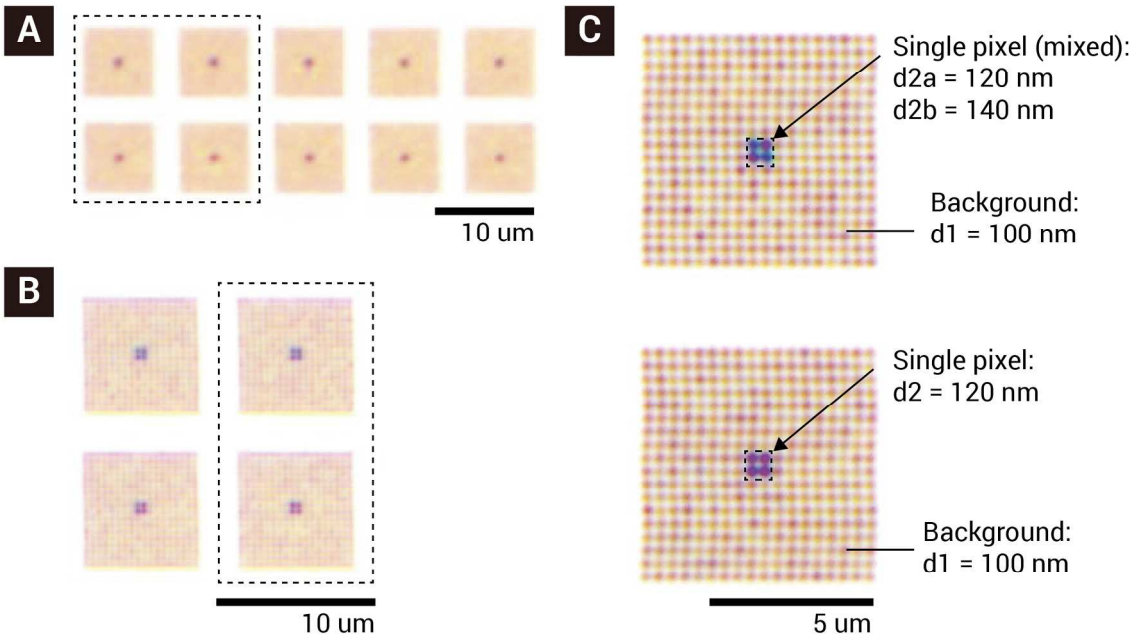

Figure S4. A single pixel of aluminum nanodisks with different diameters in both the mixed format (two different diameters) and the basic format (single diameter), was patterned in an array of pixels corresponding to the yellowish color from d = 100 nm. (A), (B) and (C) show how the pixel is resolved when imaged under different microscope magnifications, with the dotted boxed indicating the area that was magnified. At the highest magnifications, differences in color of individual disks due to slight variations in the geometry and size of the disks can be seen. Note also that the individual colors that comprise the mixed pixel can be resolved.

Tolerance of Color Pixels to Fabrication Errors

To test the tolerance of color pixels to fabrication errors, we fabricated an aluminum color palette with rough edges in comparison to a regular palette. The rough edges were introduced during the electron-beam lithography patterning step and aluminum was subsequently evaporated onto the developed HSQ patterns. Optical and SEM imaging of the color palettes (Figure S5) demonstrated that while color was still observed in palettes containing features with rough edges, the color was significantly subdued. There was also an increased variation in color within a single array of nanodisks of the same diameters to mimic the possible variations introduced in

the fabrication process. Based on these results, plasmonic colors can still be achieved with high-error processes for applications that do not require high contrast or a broad spectrum of colors.

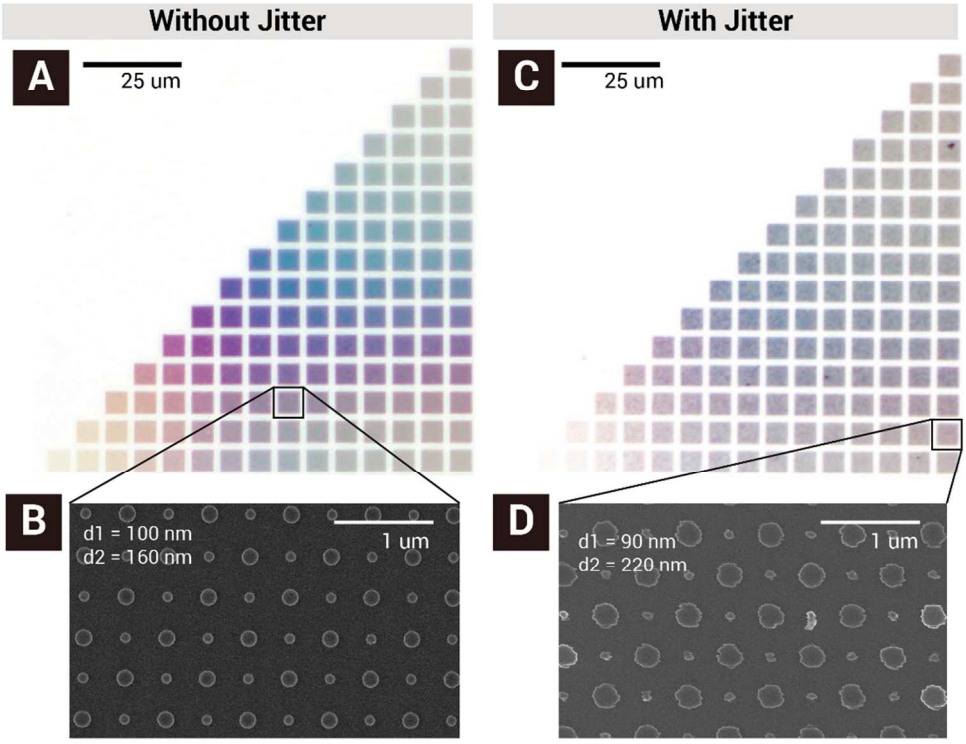

Figure S5. Tolerance of color palettes to patterning errors was tested by comparing (A, B) a regular color palette to (C, D) a color palette fabricated with rough edges. (A) and (C) are optical images while (B) and (D) are respective SEM images of pixels within each palette. These results suggest that perhaps the color purity of Al structures could be further improved by reducing edge roughness of the structures.

Experimental and Simulation Spectra for Spacing Palettes

A representative series of reflection spectra from the spacing palettes in Figure 1D was obtained using a QDI-2010 microspectrometer (CRAIC Technology), for d = 120 nm nanodisks with increasing spacing from 300 nm up to 400 nm (Figure S6). The experimental spectra was normalized against disks spaced at 250 nm apart to eliminate diffraction effects from our 800 nm pixels and instrumentation artifacts. The FDTD simulations were performed using the geometry and setup described in the Materials and Methods section of the Supporting Information (Figure

S1). The experimental spectra show a peak that increases in magnitude at ~465 nm that is not accounted for in the simulations. We believe that this peak could be an artifact of the measurements due to the inadvertent collection of diffractive orders by the microspectrophotometer. Aside from these peaks, we observed a broadening and flattening of the resonance dip at around 500 nm as the interdisk spacing decreased in both the experimental spectra and the FDTD simulations. This broadening along with a monotonic increase in reflectance intensity at the shorter wavelengths account for the subtle appearance of a bluish tint to the otherwise deep magenta color, as observed in the spacing palette under the light microscope. Given the mismatch between our simulation and experimental spectra, the spacing palettes in our pixel design may be more complex, and involves the consideration of resonances beyond individual pixels, such as surface lattice resonances.

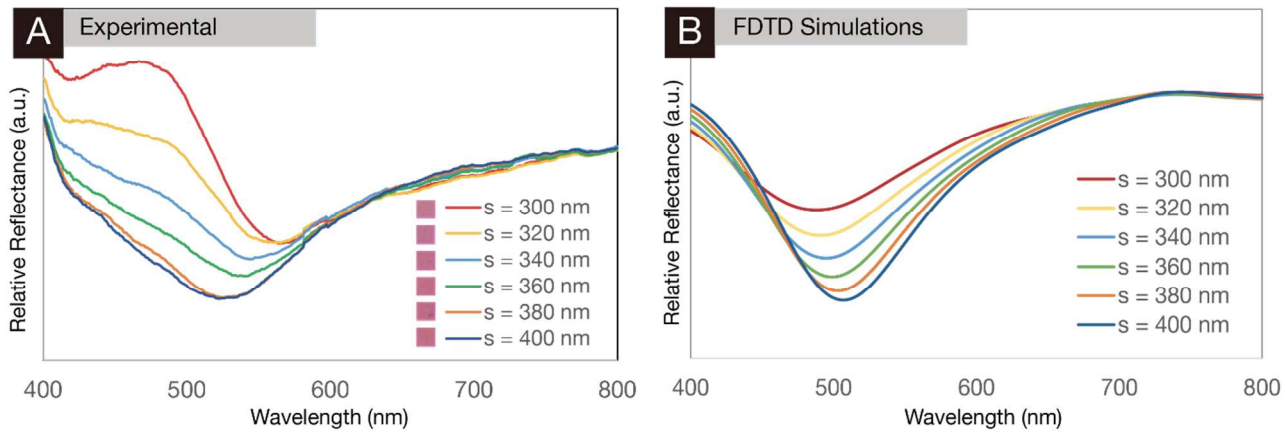

Figure S6. (A) Experimental and (B) FDTD simulations of spacing palettes for d = 120 nm, from inter-disk spacings within the plasmonic pixel of 300 to 400 nm. The presence of peaks in the experimental spectra at wavelengths < 500 nm are likely due to lattice resonances and diffraction effects that were not taken into consideration in the simulations.

Variations of Mixing and Spacing Palettes

In order to extend the plasmonic colors available, we created alternative mixing and spacing palettes with different nanodisk densities as well as different maximum spacings between

nanodisks within the pixel (Figure S7). As compared to the palettes described in the main text (four nanodisks within the plasmonic pixel with a maximum center-to-center spacing between nanodisks of 400 nm), these palettes contain nine nanodisks within the plasmonic pixel, with diameters ranging from 80 to 140 nm at steps of 5 nm and a maximum center-to-center spacing between nanodisks of 200 nm. For the mixing palettes, the plasmonic pixel contained two different sizes of nanodisks that were patterned alternating with each other at a center-to-center pitch of 200 nm. For the spacing palettes, the plasmonic pixel contained nine identical nanodisks but spaced at varying center-to-center spacing from each other, ranging from (d + 50) to a maximum distance of 200 nm.

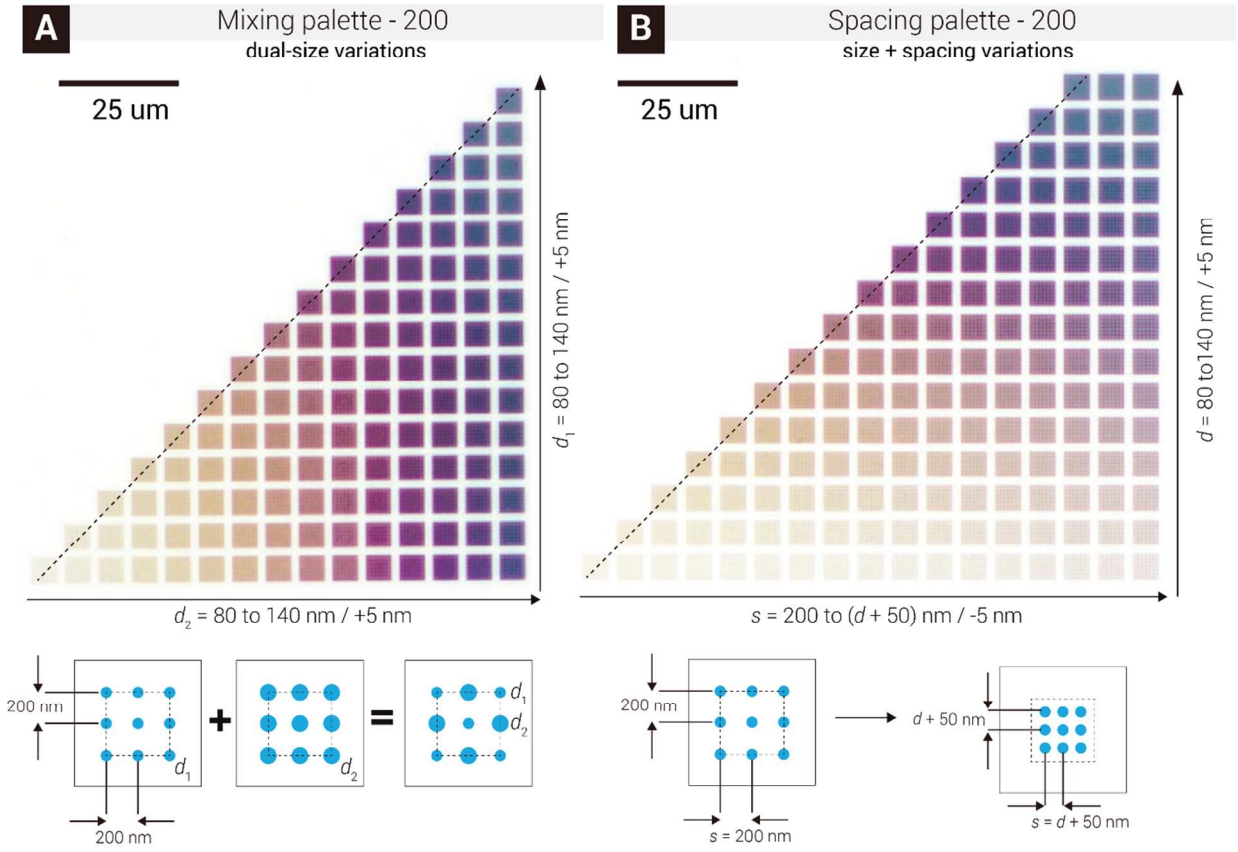

Figure S7. (A) Mixing palette containing nine nanodisks of two different diameters, positioned at a center-to-center distance of 200 nm from each other, within the plasmonic pixel area of 800 nm. The nanodisk diameters (d_1, d_2) ranged from 80 to 140 nm in steps of 5 nm. The dotted

diagonal line represents arrays of plasmonic pixels containing nanodisks of a single diameter. (B) Spacing palette containing nine nanodisks of a single diameter, but with varying center-to-center distances within the plasmonic pixel area. The diameters (d) vary from 80 to 140 nm in steps of 5 nm, which the center-to-center distances varied from (d + 50) to 200 nm in steps of 5 nm. Images were normalized to a white background.

Extent of colors in CIE 1931 Color Space

We plotted the colors achieved in CIE 1931 color space, using a MATLAB code that was adapted from the *ciegui* package written by Prashant Patil, available on Mathworks © File Exchange. The code mapped the RGB colors onto a CIE-XYZ color to demonstrate the dramatic improvements made in color generation (Figure S8). Interestingly, unlike existing pigment-based color spaces where secondary colors fall within boundaries defined by the primary colors, additional colors obtained by mixing plasmonic colors extend beyond the boundaries of the basic plasmonic colors. Indeed, this result suggests the posto further span a larger color space – some of these can be achieved by tweaking additional parameters, such as but not limited to nanodisk and nanopillar height, choice of metal, and morphology of nanostructures.

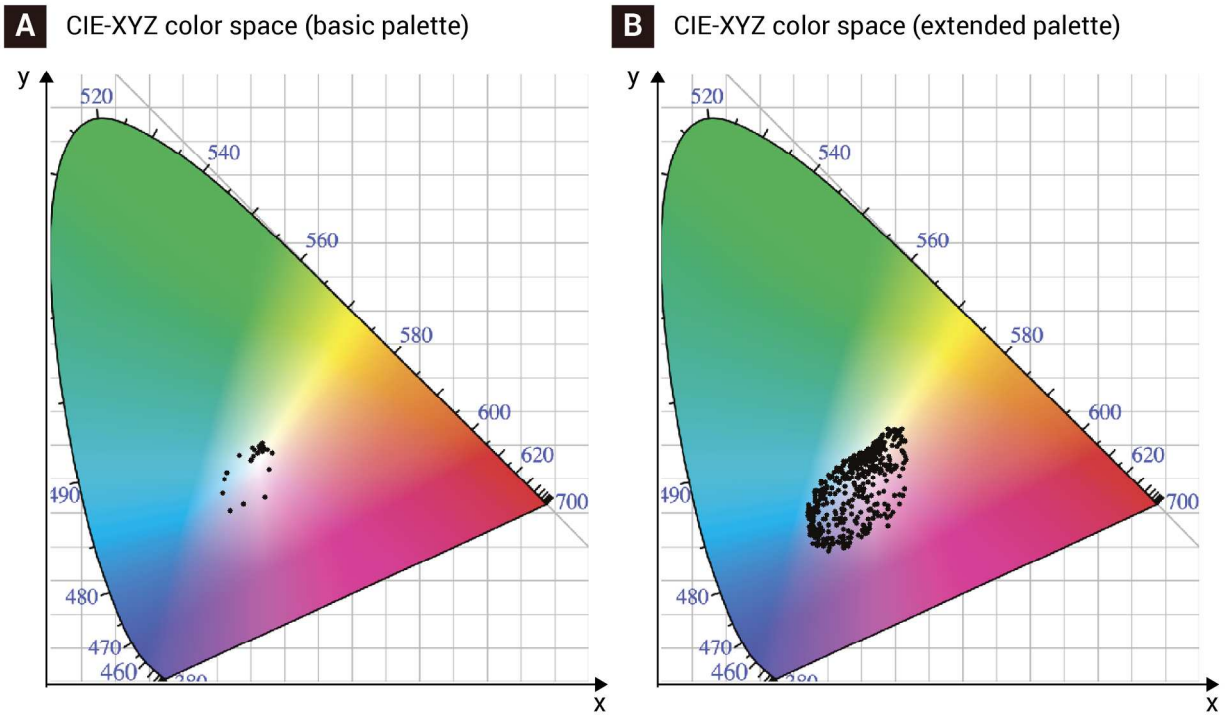

Figure S8. CIE-XYZ plots of (A) basic versus (B) extended palette.

References

(1) Yang, J. K. W.; Berggren, K. K. *J. Vac. Sci. Technol. B Microelectron. Nanom. Struct.* **2007**, *25*, 2025.

(2) Palik, E. D. *Handbook of optical constants of solids*; Academic press, 1998; Vol. 3.